Chapter 22
Estimation of Water Quality Parameters Along the Indian Coast Using Satellite Observations

Chiranjivi Jayaram, Neethu Chacko, and V. M. Chowdary

Abstract Coastal regions across the world are the most densely populated areas that exert significant pressure on the water quality of the region. The rapid urbanization and industrialization add increasingly to the pollutants that alter the coastal water quality. Operational monitoring of water quality is exhaustive and cost-sensitive exercise that is imperative for sustainable management. With the advent of numerous high-resolution satellites and open data policies being followed by various space agencies, remote sensing of water quality has become robust and an important technique for researchers and managers. Chlorophyll-*a* concentration suspended sediment concentration and turbidity are some of the water quality parameters that could be derived from the satellite observations. The present study addresses the assessment of water quality using remote sensing for selected locations along the east coast (Hooghly estuary) and the west coast (Cochin backwaters). The impact of tropical cyclone 'Bulbul' on the water quality of the Hooghly estuary and the effect of COVID-19 induced lockdown during 2020 for the Cochin backwaters are considered as case studies to demonstrate the application of satellite remote sensing in the estimation of coastal water quality parameters.

22.1 Introduction

The physical, chemical, biological and thermal characteristics of water define the water quality of a region. In general, the water quality of a particular water body is influenced by the materials discharged into it (Ritchie et al. 2003). In light of the rapid urbanization and socio-economic development (~40% of the global population) especially along the coastal regions, effective monitoring of the water quality is imperative for productive management of the coastal ecosystems (Gholizadeh et al.

C. Jayaram (✉) · N. Chacko
Regional Remote Sensing Centre—East, NRSC/ISRO, New Town, Kolkata 700156, India

V. M. Chowdary
Regional Remote Sensing Centre—North, NRSC/ISRO, Sadiq Nagar, New Delhi, India

A. Pandey et al. (eds.), *Geospatial Technologies for Land and Water Resources Management*, Water Science and Technology Library 103,
https://doi.org/10.1007/978-3-030-90479-1_22

2016). The changes that occur due to the degradation of the water quality would have an adverse impact on the fisheries and other aquatic resources of freshwater, coastal and estuarine ecosystems across the world. Some of the major pollutants that have a significant effect on the coastal water quality are the toxic chemicals released from the industries, oil spills, domestic and industrial discharge into the rivers that eventually end up in the coastal oceans. The excessive nutrients due to the fertilizers and pesticides also influence the coastal water quality (Hafeez et al. 2019). Given the importance attached to the blue economy, it is imperative to have sustained and monitoring of the water quality for nurturing the aquatic resources.

The traditional method of water quality estimation involves water sample collection at different depths of the water column and subsequent laboratory analysis of these collected samples. A systematic field campaign requires trained manpower, approach to boats/coastal. The logistics involved in safely transporting the samples from the boat to the laboratory involve huge effort and cost. Though the in-situ water sampling and measurements are accurate, they are laborious, uneconomical and inconsistent in space and time (Cai et al. 2008). These limitations of the in-situ sampling could be mitigated using remote sensing as this technology provides the data on synoptic scale at varying spatio-temporal resolutions. The advancement in remote sensing technology together with the significant enhancement in the computational resources, to process the remote sensing data, has enabled water quality monitoring to a greater extent. Ocean colour remote sensing provides information pertaining to chlorophyll-*a* concentration, total suspended matter, coloured dissolved organic matter and other water leaving spectra at different wavelengths in the visible band of the electromagnetic spectrum. The spectral characteristics of the water body like absorption, scattering, reflection, etc., are governed by the chemical and hydrobiological properties (Gholizadeh et al. 2016). The reflected radiation from the water surface is detected by the sensors mounted on various satellite platforms that are used to derive the water quality parameters from the coastal and inland water bodies.

India has a long coastline with approximately greater than 7000 km spanning nine coastal states and two island groups, along both the east and west coasts. The east coast of India is dominated by the major east flowing rivers like the Ganges, Mahanadi, Godavari, Krishna and Cauvery that carry large quantities of polluting substances that are collected in the respective watersheds. Though the west-flowing rivers are less along the western coast of India compared to the east coast, minor rivulets that originate in the western ghats and the major rivers of Narmada and Tapi would have a profound impact on the coastal water quality. In the present study, the water quality of two coastal and estuarine regions viz., the Hooghly estuary and the Cochin backwaters along the east and west coast, respectively are analysed. The impact of cyclone 'Bubul' on the Hooghly estuarine waters and the influence of COVID-19 lockdown on the Cochin backwaters are considered case studies to demonstrate the utility of remote sensing observations in water quality measurements.

22.2 Study Region

22.2.1 The Hooghly Estuary

The study focussed on the northern coastal Bay of Bengal comprising of the Hooghly estuary and the adjoining coastal areas bounded by the longitudes 87° E–89° E and latitudes 21 N–22.5° N (Fig. 22.1). This area receives a huge amount of freshwater from the Hooghly River which enters into the Bay of Bengal through the estuary. Highest river discharge is exhibited in the summer monsoon season (3000 $\pm$ 1000 $m^3\ s^{-1}$) and minimum (1000 $\pm$ 80 $m^3\ s^{-1}$) during the pre-monsoon season (Mukhopadhyay et al. 2006; Ray et al. 2015). This region is also associated with the world's largest mangrove forest, the Sundarbans and forms a part of the Gangetic delta. This region is characterised by a complex network of interconnecting channels and creeks. The other adjoining mangrove regions of the Sundarbans also receive a discharge through small rivers and channels. Therefore, the discharges into the study region greatly influence its water quality. The entire estuarine system is relatively shallow (<6 m) and is subjected to strong meso- macro tides with amplitude ranging between 5 and 7 m. The lower part of the estuarine system often experiences rough

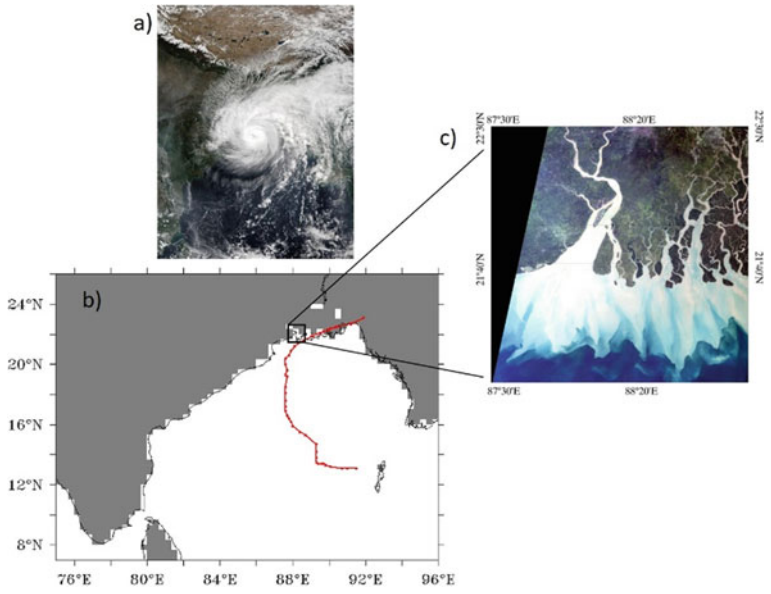

Fig. 22.1 Cyclone Bulbul and the study region. **a** True colour image of the cyclone 'Bulbul' just before it made landfall. **b** Track of the cyclone Bulbul overlaid on Bay of Bengal. The study region is marked in black rectangle. **c** The Landsat image of the study comprising Hooghly estuary and the adjoining coastal regions

weather conditions and cyclones that could strongly influence the estuarine water quality.

Bulbul was a strong and very damaging cyclone that achieved the very severe super cyclone status and struck the coast of India and Bangladesh in the year 2019. Bulbul originated as a low-pressure system over the north Andaman Sea on the 5th of November. It moved west-northwards and gained stronger winds in the next three days becoming very severe cyclone status on 8th November. On 9th November night, it made landfall on the coastal Bay of Bengal about 55 km east of Sagar Island in the Indian state of West Bengal close to the east of Sundarban Dhanchi forest with maximum sustained surface wind speed of 110–120 kmph gusting to 135 kmph. The cyclone caused heavy rains, storm surges and flash floods across the coastal region before its further weakening. The path of the cyclone Bulbul plotted using the best track data archived in the tropical cyclone database available online (http://www.rsmcnewdelhi.imd.gov.in/index.php) is shown in (Fig. 22.1).

22.2.2 Cochin Backwaters/Vembanad Lake System

The Cochin backwaters region (Lats. 9° 30′ N–10° 15′ N and Longs. 76° E–76° 30′ E) is a complex network of interconnected lagoons, swamps and canals that drain into a lake system called Vembanad Lake that extends up to 97 km in length and encompassing an area of over 300 km^2. This estuary, the third largest coastal wetland ecosystem in India, is a Ramsar site. This system has two openings to the Arabian Sea, one in the north known as the Azhikode inlet, which is narrow with a width of about 250 m and the other a more important one with a width of ~ 450 m, in the middle that acts as the entrance to the Cochin port (Vishnu et al. 2018). The Cochin estuarine region is subjected to heavy siltation, which necessitates continuous dredging to maintain channel depths suitable for navigation. Deepening of estuary by dredging increases estuary volume and alters the mixing processes and circulation patterns. Maximum load of suspended material occurs during the monsoon season, decreasing progressively during the post-monsoon periods. The nutrient load into the estuary is fed by the runoff of riverine and agricultural wastes as well as the discharge of municipal waste from the adjoining Cochin city (Shivaprasad et al. 2013a).

The Cochin backwater system is subjected to heavy pollution from the major cosmopolitan industrial city of Kochi that has a population of ~1.5 million and is a hub for more than 60% of the major chemical industrial units of the state of Kerala. Apart from the major port, the northern region of the estuary is also greatly affected by industrial activities in the Cochin shipyard, Kochi Refineries, fertilizer units and a host of medium and small-scale industrial clusters. The effluents that get drained into the estuary have a significant impact on the water quality. Similarly, in the southern region, the paddy fields and aquaculture alter the water quality of the backwaters. Indiscriminate use of fertilizers, pesticides and municipal waste generated in the Kochi city contributes about 104×10^3 m^3 of industrial waste and 260 m^3 of untreated domestic waste along with the agricultural wastes into the estuary per day (Thasneem

et al. 2018). However, due to the rapid increase of COVID-19 cases in the state of Kerala since late February 2020, the industrial output and tourism activity around the lake had significantly reduced well ahead of the national lockdown enforced from 25th March 2020. Given the composition and levels of the effluents that are getting discharged into the backwater system, the lockdown substantially reduced the stress on the ecosystem (Yunus et al. 2020). This phenomenon is expected to lead to near-natural conditions in the backwaters (Saraswat and Saraswat 2020).

22.2.3 Data and Methods

Landsat-8 Operational Land Imager (OLI), Level-1C and Sentinel-2, Multi-Spectral Instrument (MSI), Level-1C, data sets were used in this study for extracting the water quality parameters. The level-1C product is orthorectified top-of-atmosphere reflectance data with sub-pixel multispectral registration. Landsat-8 has a temporal resolution of 16 days and a spatial resolution of 30 m in the visible region. To assess the impact of tropical cyclone induced rainfall on the Hooghly estuarine region, two Landsat-8 OLI level 1 image of 2019 covering the Hooghly estuary region during the last week of October to 1st fortnight of November for path = 139/row = 47 was downloaded from the USGS online archive Earth Explorer (https://earthexplorer.usgs.gov/). (i) The image on 29th October 2019 corresponds to the pre-cyclone conditions and (ii) the image on 14th November 2011 corresponds to the post-cyclone conditions. The impact of COVID-19 lockdown on the water quality of the Cochin backwaters was studied using Sentinel-2 imagery. Data for the period 2018–2020 are used in the present study. The entire study area is covered with two scenes of MSI images (T43PFL and T43PFM). Fifty-eight images were downloaded from the Copernicus Open Access Hub (https://scihub.copernicus.eu/) during the study period. A total of 38 images were used for the analysis after screening the data for the presence of cloud and sun glint. The details of the data are provided in Table 22.1.

The processing of the Landsat optical data is done on ENVI platform. The Landsat level 1 images downloaded are undergone system radiation correction and geometry

Table 22.1 Data availability for each month/year during the study period

Date of images	2018			2019				2020				
	Feb	Mar	Apr	Feb	Mar	Apr	May	Jan	Feb	Mar	Apr	May
	03rd	05th	04th	03rd	10th	04th	29th	5th	18th	19th	3rd	3rd
	13th	10th	09th	08th	15th	09th			28th	24th	28th	
	18th	15th	19th	18th	25th							
	28th	20th	24th									
			29th									

Dates that are underlined correspond to the screened-out images

correction. The level images were processed in two steps: (1) calibration and (2) atmospheric correction. The Level 1 Landsat images were subjected to radiometric calibration for converting calibrated digital numbers into absolute units of at-sensor spectral radiance at each spectral band. The radiometrically calibrated images were then atmospherically corrected using the Fast Line-of-sight Atmospheric Analysis of Spectral Hypercubes (FLAASH) mode. The atmospheric correction eliminated the influence of atmospheric absorption and scattering. The FLAASH module facilitates automated atmospheric correction over water using NIR and SWIR channels. This is followed by elimination of cloud contaminated pixels using reflectance thresholding approach. After the cloud masking, land masking is done by using the shapefile of the Indian subcontinent. Atmospheric correction for Sentinel 2 was carried out using the ACOLITE software package (Version 20190326.0). ACOLITE was developed by the Royal Belgian Institute of Natural Science (RBINS) that employs dark spectrum fitting (DSF) method (Vanhellemont and Ruddick 2018) and (Vanhellemont 2019). The ACOLITE package computes the scattering due to aerosols using the Rayleigh-corrected reflectance for near infrared (NIR) bands in case of clear waters and shortwave infrared (SWIR) bands for turbid waters as the contribution of water towards reflectance is negligible in these bands (Martins et al. 2017). The glint correction includes the bands and pixels with the least estimate of aerosol optical thickness over the corresponding scene. This method allows the path reflectance that is insensitive to the sun glint (Vanhellemont 2019).

The reflectance bands are used to estimate TSM, turbidity and chlorophyll concentration employing the following algorithms. The algorithms used in this study are based on the single band turbidity and TSM algorithms which are functions of reflectance for the coastal waters. Total suspended matter (TSM) was derived following the retrieval algorithm developed by (Nechad et al. 2010)—water leaving reflectance of Red band ($\lambda = 665$ nm) was used to obtain the TSM from the expression (Eq. 22.1).

$$\text{TSM} = \frac{A\rho_w}{1 - \frac{\rho_w}{C}} \tag{22.1}$$

where, ρ_w is the water leaving reflectance (666 nm); A and C are the empirical coefficients obtained from (Nechad et al. 2010). The TSM thus retrieved has a root mean square error of < 10 mg/l.

Similarly, turbidity is derived from the following expression (Nechad et al. 2009):

$$\text{Turbidity} = \frac{A \cdot \rho_w}{1 - \frac{\rho_w}{C}} (\text{FNU}) \tag{22.2}$$

Chlorophyll-*a* was derived using the OC2 algorithm (Eq. 22.2) with the coefficients suggested by (Franz et al. 2015; Nazeer et al. 2020).

$$\text{Chlorphyll-a} = 10^{(0.1977 - 1.8117R + 1.9743 * R^2 - 2.5635 * R^3 - 0.7218 * R^4)}. \tag{22.3}$$

where, R is the ratio of blue-green bands, which are 442 nm and 560 nm (S2A)/559 nm (S2B). The accuracy of OC2 algorithm for the Indian coastal waters is <0.73 mg m^{-3} (Poddar et al. 2019).

22.3 Variability of the Water Quality Parameters in the Hooghly Estuary

Estimates of the three important water quality parameters: TSM, turbidity and chlorophyll concentration are obtained from the atmospherically corrected surface reflectance. Figure 22.2 shows the TSM values before and after the cyclone. Fig. 22.2a forms the background conditions of the TSM based on which the impact of the cyclone Bulbul can be assessed. It can be seen that the pre-cyclone TSM concentration was lower in the entire coastal regions ranging from 20 to 30 g/m^3 in the mouth of the Hooghly estuary, increasing upstream with values reaching up to 35–40 g/m^3 in the upper estuary. The areas in the adjoining coastal regions and in the creeks of the Sundarbans, the TSM is much lower in the range 10–20 g/m^3. In the offshore regions, the TSM values are generally below 5 g/m^3. The concentration of TSM within the Hooghly estuary has a spatial distribution characteristic of high in the upstream and low in the downstream. Post-bulbul, it can be observed from Fig. 22.2b that the concentration of TSM increases in the study region. The elevation in the concentration of TSM is pronounced within the Hooghly estuary than elsewhere. The satellite observations reveal a large spatial extent of the higher TSM distribution, suggesting

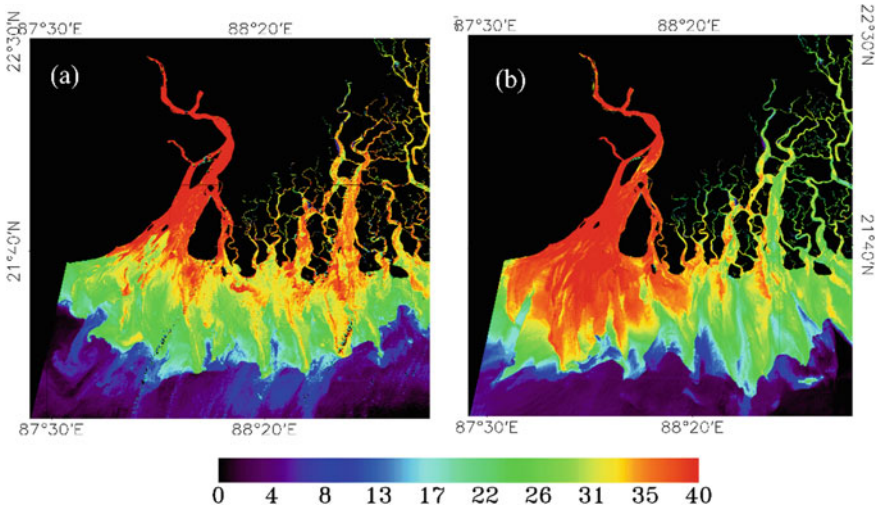

Fig. 22.2 Maps of Total suspended matter (g/m^3) estimated from Landsat-8: (a) before cyclone 'Bulbul' (29th October 2019) and (b) after cyclone 'Bulbul' (14th November 2019)

a strong impact of the cyclone on the TSM. The TSM concentration ranges between 40 and 45 g/m^3 in the entire Hooghly estuary towards the estuary mouth. The values of TSM concentration in the adjoining coastal regions also increased to 25–30 g/m^3. The highest change in TSM concentration occurred within the Hooghly estuary and its mouth where the tongues of higher TSM can be seen flushing out into the offshore waters.

The impact of the cyclone Bulbul on the water turbidity is shown in Fig. 22.3. Before the cyclone, the turbidity values in the coastal and offshore regions were low, while values increased in the Hooghly region. Within the Hooghly estuary, the turbidity was relatively higher particularly in the shallower northern upper estuary (Fig. 22.3a).

The plumes of turbidity high observed in the upper estuary range in concentration from 275 to 300 FNU which seem to be primarily related to the higher TSM concentration prevailed before the cyclone. The pre-cyclone turbidity in the regions outside the estuary and within the creeks of Sundarbans (70–80 FNU). Post-cyclone, the turbidity values are increased inside the estuary ranging from 300 to 400 FNU. The turbidity values in the offshore regions also exhibit a slight increase in turbidity after the passage of Bulbul. It can be observed that a significant increase in the turbidity happened inside the Hooghly estuary than elsewhere. The overall pattern in the variation of turbidity is similar to that of the TSM which points out the contribution of TSM in increasing turbidity in the dynamic Hooghly estuary.

Impact of cyclone Bulbul on the chlorophyll concentration in the northern coastal Bay of Bengal is shown in Fig. 22.4. Before Bulbul (Fig. 22.4a) made its landfall, the chlorophyll concentration was generally high within the Hooghly estuary and

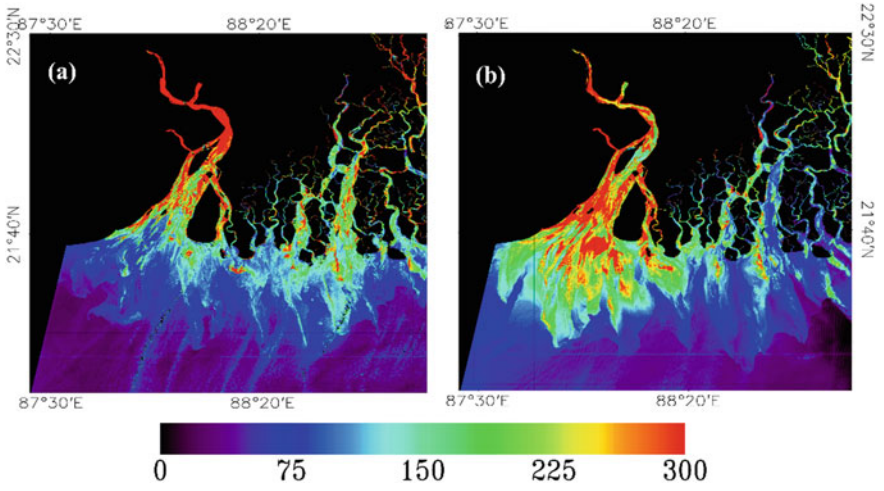

Fig. 22.3 Maps of turbidity (FNU) estimated from Landsat-8 **a** before Bulbul (29th October 2019) and **b** after Bulbul (14th November 2019)

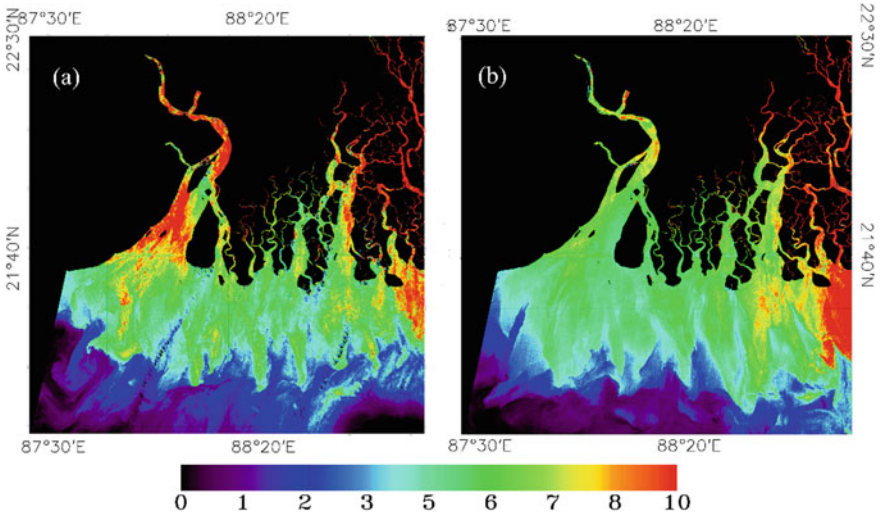

Fig. 22.4 Maps of chlorophyll concentration (mg/m^3) estimated from Landsat-8 **a** before Bulbul (29th October 2019) and **b** after Bulbul (14th November 2019)

in the creeks in the Sundarbans located in the eastern part of the study region (~7–10 mg/m^3). Filaments of chlorophyll-rich waters can be observed as emanating from the creeks and estuary towards the open ocean. The landfall of the Bulbul apparently caused an interestingly different pattern of chlorophyll concentration (Fig. 22.4b) than the other two parameters. In the Hooghly estuary and adjacent creeks and channels, the chlorophyll concentration is observed as decreasing after the cyclone Bulbul. The chlorophyll concentration decreased to ~6–7.5 mg/m^3 as compared to the pre-cyclone values >7–10 mg/m^3. Many studies have reported on the increase of chlorophyll concentration in the aftermath of cyclones (Subrahmanyam et al. 2002; Babin et al. 2004; Chacko 2017, 2019). But in this case, a clear large spatial scale reduction of chlorophyll concentration occurred except in the eastern part of the study region. A visual comparison of the variability of post-cyclone TSM, turbidity and chlorophyll concentration reveal that the decrease in the chlorophyll concentration happened over the regions where there is an increase in the concentration of TSM and turbidity.

The discharge and the resuspension induced by the physical forcing introduce a large amount of nutrients into the water column. Shelby et al. (2006) reported that the input of nutrients after major hurricanes was almost equal to the average annual input over several years. Williams et al. (2008) showed that total organic carbon, ammonium and other soluble reactive phosphorous concentrations increased two to five times after the passage of a series of hurricanes in Florida Bay. The increased input of nutrients into the region can have a profound impact in increasing the phytoplankton biomass by increasing the photosynthesis mechanism (Havens et al. 2012). However, the increased river discharge and mixing have a huge impact on the penetration of light into the water column. As a result of these, there will be

an increase in the light attenuating substances in the water column which reduces the overall clarity of the water in the coastal systems. Light and nutrient availability are the major limiting factors for the chlorophyll concentration in the open ocean as well as coastal waters (Chacko 2017). Though nutrient input increases in the coastal waters which can support the algal growth, without sufficient light penetration, the production of biomass will be retarded.

Studies by Manna et al. (2010), Mitra et al. (2009) and Roshith et al. (2018) points that Hooghly estuary remains eutrophic throughout the year. This implies that the chlorophyll concentration remains high in the estuary as shown in Fig. 22.4a due to the high nutrient load from river discharges (Roshith et al. 2018). Havens et al. (2011) had examined that in eutrophic waters, an increase in the nutrient load due to flood water surge will not result in an increase in biomass as it would impact oligotrophic waters. In oligotrophic and open oceanic regions, however, the impacts of cyclones result in the entrainment of nutrients which are limited in the upper near surface waters, thereby increasing the chlorophyll concertation by new production (Gierach and Subrahmanyam 2008; Chacko 2017). Thus, in eutrophic waters like Hooghly estuary, light penetration plays a major role in determining the phytoplankton biomass. Similar Observations are made by Mallin et al. (2002) and Srichandan et al. (2015) indicating the importance of light limitation in inducing the changes of chlorophyll concentration in coastal environments where nutrients are abundant.

22.4 Impact of COVID-19 Lockdown on the Cochin Backwaters

22.4.1 Average of TSM and Chlorophyll-a in the Study Region

The three year mean of TSM was computed for the months of February—April as shown in Fig. 22.5. Based on the TSM concentration from the figure, it is evident that the backwater system could be categorised into the northern region and the southern region. The sediment concentration is higher (~40 g m^{-3}) in the northern part than in the southern part (~15 g m^{-3}) during all three months with higher values observed in April. The patches of high sediment concentration observed in the southern region arise from the Kuttanad paddy fields. There are two reasons for the relatively high concentration in the northern region: (1) One of the openings into the ocean is the bar mouth area or the Cochin inlet, where there is a constant interaction between the ocean waters and the backwaters. The tidal forces churn the subsurface thereby increasing the suspended sediments. (2) The presence of active port and Naval facilities in Cochin city requires regular dredging activities to maintain the channel depth for safe navigation. Dredging resuspends the sediments deposited on the seabed.

The three year mean of chlorophyll-*a* (Fig. 22.6) exhibited a gradual decrease

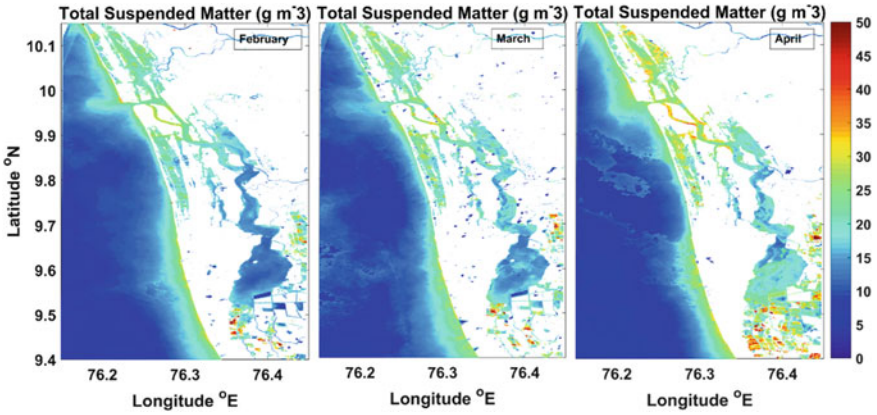

Fig. 22.5 Three year mean of TSM for the months of February, March and April

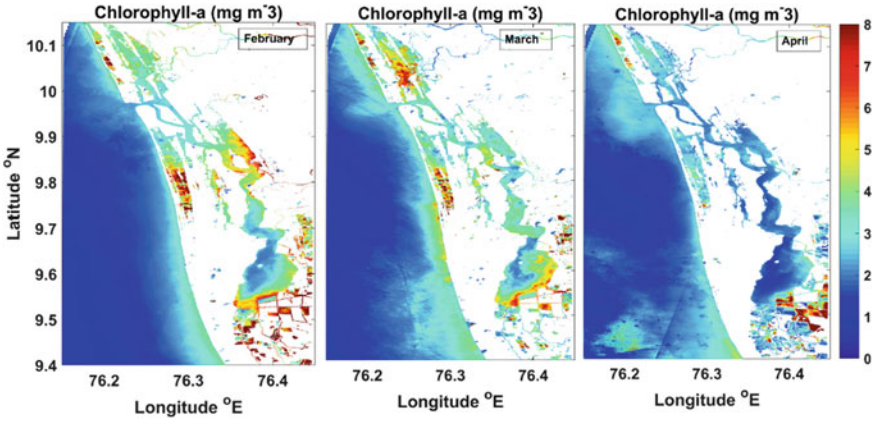

Fig. 22.6 Three year mean of Chlorophyll-*a* for the months of February, March and April

from February (high in the middle of the estuary with values <2 mg m^{-3}) to April (>5 mg m^{-3}) across the region except for the few patches in the southern region that is dominated by the paddy fields of Kuttanad region. The waters are generally oligotrophic due to little precipitation and river runoff during the pre-monsoon season that is evident in April when the entire coastal region and backwaters are observed to have relatively lower chlorophyll concentrations. The average surface chlorophyll-*a* of the backwater system during the pre-monsoon season is less than 3 mg m^{-3} going on *in-situ* observations of (Shivaprasad et al. 2013b) that are corroborated the satellite data.

22.4.2 TSM During the Lockdown Period

Monthly mean TSM and chlorophyll-*a* were mapped for the months of February—April 2020 with the February data coming from the pre-lockdown period, the March observations representing the initial/preparation phases of lockdown and April the data representing the peak of the lockdown (Fig. 22.7). The monthly values clearly depict the impact of reduced pollutant levels on the surface water quality of the entire Cochin backwater system, especially near the Cochin inlet and southern part of the study area.

To avoid the ambiguity due to the interannual variability, the monthly anomalies were computed for these three months as shown in Fig. 22.8. It is observed that the TSM concentration decreased by ~10 g m^{-3} during March and April near the

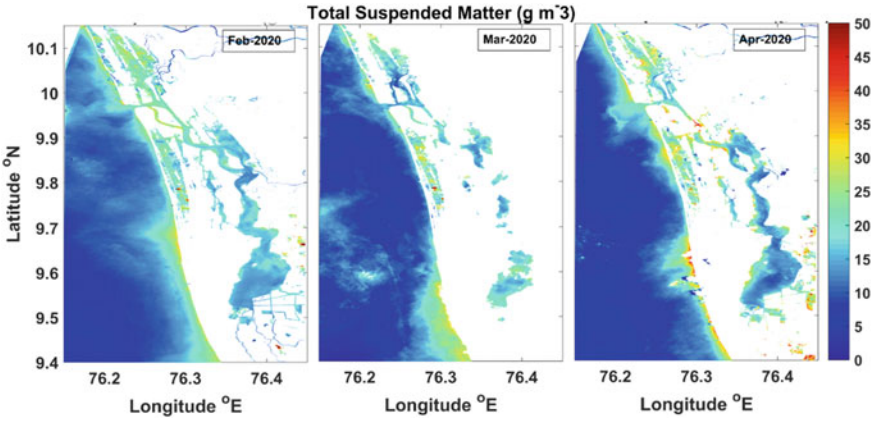

Fig. 22.7 Monthly mean of TSM for February, March and April 2020

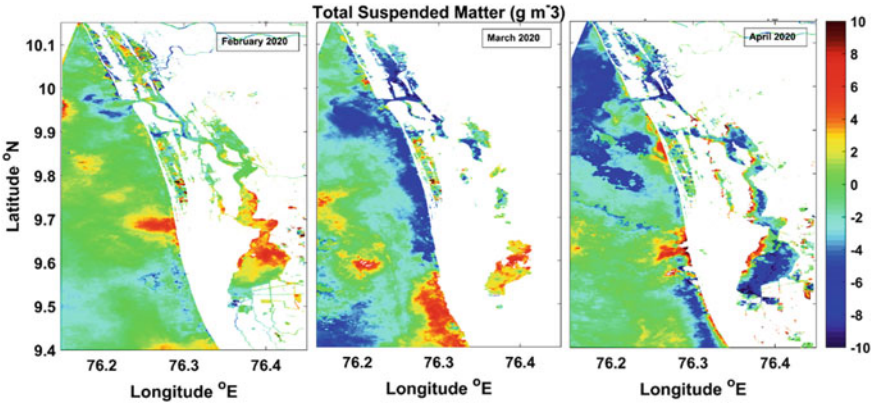

Fig. 22.8 Monthly anomaly of TSM for February, March and April 2020

Cochin inlet that could be attributed to the reduced ship traffic in March and complete lockdown in April. However, the southern region showed a positive anomaly in March, indicating the continuation of farming activities in the region prior to the lockdown period. The TSM in the entire study region showed negative anomalies in April when the lockdown impact was at its maximum. Positive or non-negative anomalies are observed at a few places very close to the land–water boundary that could be attributed to sewage discharge in the region. This infers the contribution of industrial discharge on the total suspended matter concentration of the estuarine region during pre-monsoon season when the runoff is at its minimum.

22.4.3 *Chlorophyll-a Concentration During the Lockdown Period*

Mean chlorophyll-*a* concentrations for February–April 2020 is shown in Fig. 22.9. Chlorophyll-*a* in the estuary varied between 1 and 8 mg m^{-3}. Chlorophyll-*a* was relatively high to the north of the Cochin inlet and at the southern fringes of the study region both in February and March with the highest concentration is observed in March to the north of Cochin inlet. The chlorophyll-*a* concentration in April is comparatively lower all along the estuary with values ranging from 1 to 3 mg m^{-3}. To ascertain the increase in the chlorophyll-*a* concentration, the monthly chlorophyll anomaly is mapped in Fig. 22.10.

The chlorophyll anomaly in February 2020 is negative towards the southern region of the estuary and positive in the northern part. During the month of March, anomalously high chlorophyll-*a* concentration is observed all over the backwaters with positive anomalies up to 2 mg m^{-3}. During the lockdown month of April, positive anomalies are observed in the Cochin inlet and the southern fringes of the estuary.

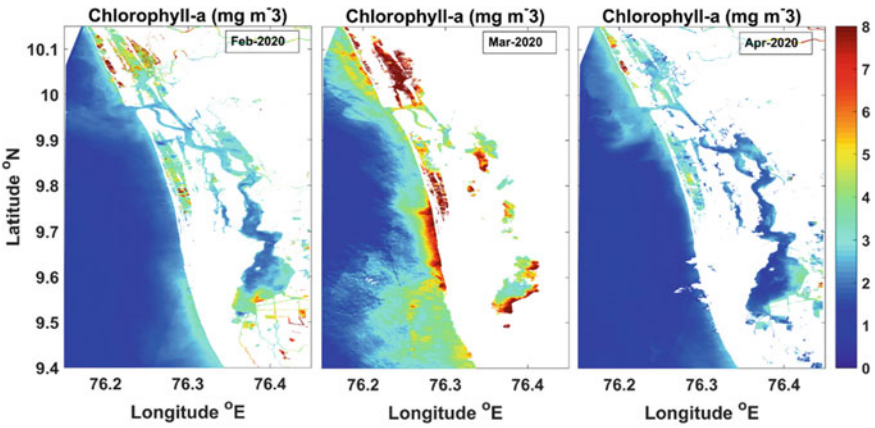

Fig. 22.9 Monthly mean of chlorophyll-*a* for February, March and April 2020

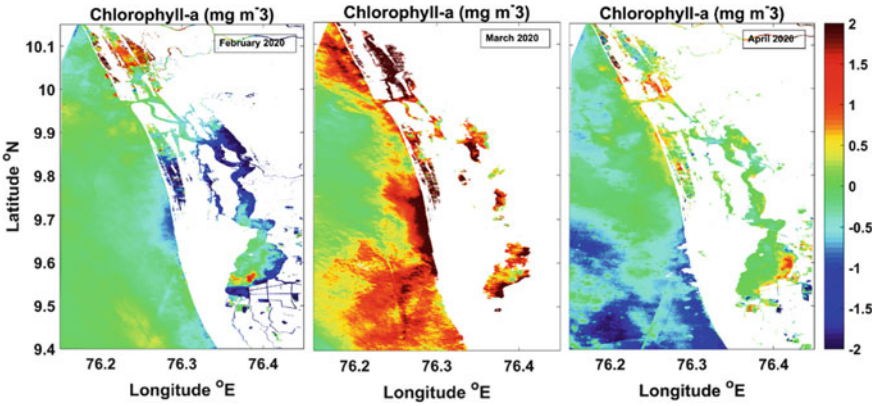

Fig. 22.10 Monthly anomaly of chlorophyll-*a* for February, March and April 2020

The positive anomalies in March and April could be attributed to the reduction in the TSM concentration during these two months thus allowing increased penetration of light that enhanced the productivity of the region. This is further supported by the lack of positive anomalies of chlorophyll during March, April of 2018 and 2019, respectively.

22.4.4 Influence of Tides on TSM and Chlorophyll-a in the Cochin Backwaters

The TSM concentration increases during the high tide as the bottom sediments get churned thereby resulting in their resuspension as evident from high concentration of TSM in the satellite imagery. In order to check the influence of tide on the suspended sediment distribution of the region, the hourly tide data near the bar mouth region was obtained from Cochin Port Trust. The time of satellite pass over the study region is observed to be between 0506 and 0508 h UTC that is approximately 1036-1038 IST. As per the available tide data, the low tide is observed between 1000 and 1100 h IST, for the dates (March 19th, April 3rd and 28th, May 3rd of 2020) on which the satellite data are available. Therefore, the influence of tide on the TSM concentration would be small and the observed TSM concentration and chlorophyll-*a* must result from lockdown.

22.5 Conclusions

The present study demonstrates the application of remote sensing technologies to assess the water quality along the Indian coast through two case studies viz., the

effects of tropical cyclones on the water quality parameters of the northern coastal Bay of Bengal and the impact of COVID-19 lockdown on the Cochin backwaters. The parameters that were considered as proxies of water quality are the TSM, turbidity and chlorophyll.

High-resolution images from Landsat-8 were used to characterise the impact of cyclone 'Bulbul' on the water quality of the Hooghly estuary and the adjoining coastal areas comprising the Sundarbans. The observations of TSM, turbidity and chlorophyll concentration before and after Bulbul showed that the water quality of the coastal system deteriorated due to the cyclone. The strong rainfall associated with the cyclone induced high surface runoff into the study area which resulted in bringing large number of suspended solids and reduced the water clarity. The increase in TSM and the turbidity greatly deteriorated the light penetration of the water column. Decreased light penetration due to increased turbidity is implicated as the plausible reason which resulted in the observed decrease in chlorophyll concentration. This study shows that in the eutrophic estuarine systems like Hooghly, the algal growth is strongly dependent on light availability and any factor which can reduce the light availability can reduce the phytoplankton biomass in the region.

The impact of COVID-19 lockdown on the estuarine water quality is elucidated in Cochin backwaters as a case study. The TSM and chlorophyll-*a* concentration are considered in this study to assess the impact of the lockdown period of April 2020 on water quality. Satellite imagery from Sentinel-2/MSI is used to derive TSM and chlorophyll during February–April for the years 2018–2020. Monthly means and anomalies of TSM and chlorophyll are generated to determine the anomalous values during March and April 2020. The TSM is observed to fall by 10 g m^{-3} especially in the Cochin inlet region, where relatively high turbid waters prevail owing to the port activities and discharge of industrial and municipal wastes into the region. Th COVID-19 lockdown has led to remarkable improvement in water quality including an increase in chlorophyll due to deeper light penetration. This study emphasises the influence of anthropogenic activities on the coastal water quality and throws light on the need for pollution mitigation for sustainable development with cleaner coasts.

Acknowledgements Authors thank the USGS and ESA for making available the Landsat—8/OLI and Sentinel-2 A/B datasets. We are also thankful to the RBIN team for the development and distribution of the ACOLITE package. Authors thank the Head (Applications) and the General Manager, RRSC-East for the support.

References

Babin SM, Carton JA, Dickey JA, Wiggert JD (2004) Satellite evidence of hurricane-induced phytoplankton blooms in an oceanic desert. J Geophys Res 109:C03043. https://doi.org/10.1029/2003JC001988

Cai L, Liu P, Zhi C (2008) Discussion on remote sensing based on water quality monitoring methods. Geomat Spat Inf Technol 31:68–73. https://doi.org/10.3969/j.issn.1672-5867.2008.04.021

Chacko N (2017) Chlorophyll bloom in response to tropical cyclone Hudhud in the Bay of Bengal: Bio-Argo subsurface observations. Deep Sea Res 1(124), 66–72. https://doi.org/10.1016/j.dsr.2017.04.010

Chacko N (2019) Differential chlorophyll blooms induced by tropical cyclones and ther relation to cyclone characteristics and ocean pre-conditions in the Indian Ocean. J Earth Syst Sci 128:177. https://doi.org/10.1007/s12040-019-1207-5

Franz BA, Bailey SW, Kuring N, Werdell JP (2015) Ocean color measurements with the Operational Land Imager on Landsat-8: implementation and evaluation in SeaDAS. J Appl Remote Sens 9, 096070. https://doi.org/10.1117/1.JRS.9.096070

Gholizadeh MH, Melesse AM, Reddi L (2016) A comprehensive review on water quality parameters estimation using remote sensing techniques. Sensors 16:1298. https://doi.org/10.3390/s16081298

Gierach MM, Subrahmanyam B (2008) Biophysical responses of the upper ocean to major Gulf of Mexico hurricanes in 2005. J Geophys Res 113:C04029. https://doi.org/10.1029/2007JC004419

Hafeez S, Wong MS, Abbas S, Kwok CYT, Nichol J, Lee KH, Tang D, Pun L (2019) Detection and monitoring of marine pollution using remote sensing technologies. In: Fouzia HB (ed) Monitoring of marine pollution. IntechOpen. https://doi.org/10.5772/intechopen.76739

Havens KE, Beaver JR, Casamatta DA, East TL, James RT, Mccormick P, Phlips EJ, Rodusky AJ (2011) Hurricane effects on the planktonic food web of a large subtropical lake. J Plankton Res 33:1081–1094

Mallin MA, Posey MH, McIver MR, Parsons DC, Ensign SH, Alphin TD (2002) Impacts and recovery from multiple hurricanes in a Piedmont-coastal plain river system. Biosciences 52:999–1010

Manna S, Chaudhuri K, Bhattacharya S, Bhattacharya M (2010) Dynamics of Sundarban estuarine ecosystem: eutrophication induced threat to mangroves. Aquat Biosyst 6:8. https://doi.org/10.1186/1746-1448-6-8

Martins VS, Barbosa CCF, DeCaralho LAS, Jorge DSF, Lobo FDL, Novo EML (2017) Assessment of atmospheric correction methods for sentinel-2 MSI images applied to Amazon flood plain lakes. Remote Sens 9:322. https://doi.org/10.3390/rs9040322

Mitra A, Gangopadhayay V, Dube A, Schmidt ACK, Banerjee K (2009) Observed changes in water mass properties in the Indian Sundarbans (north-western Bay of Bengal) during 1980–2007. Curr Sci 97:1445–1452

Mukhopadhyay SK, Biswas H, De T, Jana TK (2006) Fluxes of nutrients from the tropical River Hooghly at the land-ocean boundary of Sundarbans, NE Coast of Bay of Bengal. J Mar Syst 62:9–21. https://doi.org/10.1016/j.jmarsys.2006.03.004

Nazeer M, Bilal M, Nichol JE, Wu W, Alsahli MMM, Shahzad MI et al (2020) First experiences with the Landsat-8 aquatic reflectance product: evaluation of the regional and ocean color algorithms in a coastal environment. Remote Sens 12:1938

Nechad B, Ruddick KG, Neukermans G (2009) Calibration and validation of a generic multi sensor algorithm for mapping of turbidity in coastal waters. In: Ch R Bostater SP Jr, Mertikas XN, Velez-Reyes M (eds) SPIE, remote sensing of the ocean, sea ice, and large water regions, vol 7473. Berlin, Germany, p 74730H

Nechad B, Ruddick K, Park Y (2010) Calibration and validation of a generic multi-sensor algorithm for mapping of total suspended matter in turbid waters. Remote Sens Environ 114:854–866. https://doi.org/10.1016/j.rse.2009.11.022

Poddar S, Chacko N, Swain D (2019) Estimation of chlorophyll-a in the northern coastal Bay of Bengal using Landsat-8 OLI and Sentinel-2 MSI sensors. Front Mar Sci 6:598. https://doi.org/10.3389/fmars.2019.00598

Ray R, Rixen T, Baum A, Malik A, Gleixner G, Jana TK (2015) Distribution, sources and biogeochemistry of organic matter in a mangrove dominated estuarine system (Indian Sundarabans) during the pre-monsoon. Estuarine Coastal Shelf Sci 167:404–413. https://doi.org/10.1016/j.ecss.2015.10.017

Ritchie JC, Zimba PV, Everitt JH (2003) Remote sensing techniques to assess water quality. Photogramm Eng Remote Sens 69:695–704

Roshith CM, Meena DK, Manna RK, Sahoo AK, Swain HS, Raman RK, Sengupta A, Das BK (2018) Phytoplankton community structure of the Gangetic (Hooghly-Matla) estuary: status and ecological implications in relation to eco-climatic variability. Flora 240:133–143. https://doi.org/10.1016/j.flora.2018.01.001

Saraswat R, Saraswat DA (2020) Research opportunities in pandemic lockdown. Science 368:594–595. https://doi.org/10.1126/science.abc3372

Shelby JD, Chescheir GM, Skaggs RW, Amatya DM (2006) Hydrologic and water quality response of forested and agricultural lands during the 1999 extreme weather conditions in Eastern North Carolina. Am Soc Agricult Eng 48:2179–2188

Shivaprasad A, Vinita J, Revichandran C, Reny PD, Deepak MP, Muraleedharan KR, Naveen Kumar KR (2013a) Seasonal stratification and property distributions in a tropical estuary (Cochin estuary, west coast, India). Hydrol Earth Syst Sci 17:187–199. https://doi.org/10.5194/hess-17-187-2013

Shivaprasad A, Vinita J, Revichandran C, Manoj NT, Srinivas K, Reny PD, Ashwini R, Muraleedharan KR (2013b) Influence of saltwater barrage on tides, salinity and chlorophyll-a in Cochin estuary, India. J Coastal Res 29:1382–1390. https://doi.org/10.2112/JCOASTRES-D-12-00067.1

Srichandan S, Kim JY, Kumar A, Mishra DR, Bhadury P, Muduli PR, Pattnaik AK, Rastogi G (2015) Interannual and cyclone-driven variability in phytoplankton communities of a tropical coastal lagoon. Mar Pollut Bull 101:39–52

Subrahmanyam B, Rao KH, Rao NS, Murty VSN, Sharp RJ (2002) Influence of a tropical cyclone on Chlorophyll-a concentration in the Arabian Sea. Geophys Res Lett 29:2065. https://doi.org/10.1029/2002GL015892

Thasneem TA, Nandan SB, Geetha PN (2018) Water quality status of Cochin estuary, India. Indian J Geo-Mar Sci 47:978–989

Vanhellemont Q, Ruddick K (2018) Atmospheric correction of metre-scale optical satellite data for inland and coastal water applications. Remote Sens Environ 216:586–597. https://doi.org/10.1016/j.rse.2018.07.015

Vanhellemont Q (2019) Adaptation of the dark spectrum fitting atmospheric correction for aquatic applications of the Landsat and Sentinel-2 archives. Remote Sens Environ 225:175–192. https://doi.org/10.1016/j.rse.2019.03.010

Vishnu PS, Shaju SS, Tiwari SP, Menon N, Nashad M, Joseph CA, Raman M, Hatha M, Prabhakaran MP, Mohandas A (2018) Seasonal variability in bio-optical properties along the coastal waters off Cochin. Int J Appl Earth Obs Geoinf 66:184–195. https://doi.org/10.1016/j.jag.2017.12.002

Williams CJ, Boyer JN, Jochem FJ (2008) Indirect hurricane effects on resource availability and microbial communities in a subtropical wetland–estuary transition zone. Estuaries Coasts 31:204–214

Yunus AP, Masago Y, Hijoka Y (2020) COVID-19 and surface water quality: improved lake water quality due to the lockdown. Sci Total Environ 731:13902. https://doi.org/10.1016/j.scitotenv.2020.139012